Coupled electron–phonon transport from molecular dynamics with quantum baths

2009 J. Phys.: Condens. Matter 21 025503

(http://iopscience.iop.org/0953-8984/21/2/025503)

J. Phys.: Condens. Matter **21** (2009) 025503 (6pp) doi:10.1088/0953-8984/21/2/025503

Coupled electron–phonon transport from molecular dynamics with quantum baths

J T Lü[1] **and Jian-Sheng Wang**

Center for Computational Science and Engineering and Department of Physics,
National University of Singapore, Singapore 117542, Republic of Singapore

Received 3 September 2008, in final form 6 November 2008
Published 9 December 2008
Online at stacks.iop.org/JPhysCM/21/025503

Abstract
Based on generalized quantum Langevin equations for the tight-binding wavefunction amplitudes and lattice displacements, electron and phonon quantum transport are obtained exactly using molecular dynamics (MD) in the ballistic regime. The electron–phonon interactions can be handled with a quasi-classical approximation. Both charge and energy transport and their interplay can be studied. We compare the MD results with those of a fully quantum mechanical nonequilibrium Green's function (NEGF) approach for the electron currents. We find a ballistic to diffusive transition of the electron conduction in one-dimensional chains as the chain length increases.

(Some figures in this article are in colour only in the electronic version)

1. Introduction

The interaction of electrons with phonons in open nonequilibrium molecular structures is of great importance within the context of molecular electronics [1, 2]. A variety of methods at different levels of sophistication has been used to study this problem, each working at a specific parameter range [1, 3]. The perturbative approach with a self-consistent Born approximation (SCBA) works well when the electron–phonon interaction (EPI) is weak, and has been used in the first-principles study [4]. In the strong interaction limit, it is possible to eliminate the bilinear EPI term via a canonical transformation [5]. This latter approach is useful to study toy model systems. It can provide exact solutions only for several special cases, e.g. without direct tunneling between different electron states [6]. It is also possible to study the coherent electron–phonon dynamics in the full coupling regimes using the scattering theory [7], but this kind of method ignores dephasing between electrons and phonons. Hybrid approaches exist, where the electron part is treated quantum-mechanically, while the phonon system is handled by classical MD [8] with quantum corrections [9]. Most of the above methods are developed within the context of electronic transport. The inclusion of phonon transport appeared only very recently, mainly using the NEGF approach [10, 11].

Molecular dynamics is usually viewed as a method that produces only classical results. In this paper, we introduce a new MD method to study the coupled electron and phonon transport in open molecular junctions for the quantum systems. It is based on a generalized Langevin equation [12] for electrons and phonons, which so far has been used to study their quantum transport separately [13, 14]. The formalism is exact in the ballistic case, i.e. without the EPI. Quasi-classical approximation [15] is made to the full quantum many-body problem for interacting systems. It does not have to assume a bilinear form of the EPI Hamiltonian, and it is applicable to the full electron–phonon coupling range. More importantly, the method can simulate large systems. In the rest of the paper, we introduce a model system, derive the quantum Langevin equations, and analyze the approximation involved. We present the MD numerical results of molecular chains, and compare them with those from the NEGF method.

2. Model and theory

Consider a typical LCR structure for transport study, where a molecular structure (C) is connected with two semi-infinite leads (L and R) as electron and phonon reservoirs. The two leads are linear systems in their respective thermal equilibrium states characterized by the chemical potential and temperature. Possible many-body interactions only exist in the central region. The total Hamiltonian is the sum of the two subsystems

[1] Present address: DTU Nanotech, NanoDTU, Technical University of Denmark, 2800 Lyngby, Denmark.

and their interaction, $H_e + H_{ph} + H_{epi}$. The phonon part is

$$H_{ph} = \sum_{\alpha=L,C,R} H^{\alpha}_{ph} + (u^L)^T V^{LC}_{ph} u^C + (u^C)^T V^{CR}_{ph} u^R + V_n, \quad (1)$$

where $H^{\alpha}_{ph} = \frac{1}{2}(\dot{u}^{\alpha})^T \dot{u}^{\alpha} + \frac{1}{2}(u^{\alpha})^T K^{\alpha} u^{\alpha}$. u^{α} is a column vector consisting of all the displacement operators in the α region, and $\dot{u}^{\alpha}$ is its conjugate momentum. The atomic mass has been absorbed into $u_j = \sqrt{m_j}\, x_j$. K^{α} is the spring constant matrix. V^{LC}_{ph} is the coupling matrix between the left lead and the central molecule, and $V^{CL}_{ph} = (V^{LC}_{ph})^T$, similarly for V^{CR}_{ph}. V_n is an anharmonic potential, which only depends on u^C. The electron subsystem is given in a tight-binding form in an orthogonal basis,

$$H_e = \sum_{\alpha=L,C,R} c^{\alpha\dagger} T^{\alpha} c^{\alpha} + \sum_{\alpha=L,R} \left(c^{C\dagger} V^{C\alpha}_e c^{\alpha} + \text{h.c.} \right), \quad (2)$$

c^{α} ($c^{\alpha\dagger}$) is the column (row) vector containing all the annihilation (creation) operators in the α region. $V^{C\alpha}_e$ has a similar meaning to $V^{C\alpha}_{ph}$, and $V^{C\alpha}_e = (V^{\alpha C}_e)^{\dagger}$. h.c. represents Hermitian conjugate. The total electron energy under the Born–Oppenheimer approximation depends on the position of the atoms, so that we can make a Taylor expansion of it about the atomic equilibrium positions, and obtain the electron–phonon interaction terms (e.g. from a first-principles calculation)

$$H_{epi} = \sum_{ijk} c^{\dagger}_i M^k_{ij} c_j u_k + \tfrac{1}{2} \sum_{i,j,k,l} c^{\dagger}_i M^{kl}_{ij} c_j u_k u_l + \cdots, \quad (3)$$

H_{epi} includes all the higher order terms of the Taylor expansion. The superscript C has been omitted since EPI only takes place in the center part. M^k_{ij} and M^{kl}_{ij} are the first and second order EPI coefficients, respectively.

Working in the Heisenberg picture, we obtain the equations of motion for operators u^{α} and c^{α}, e.g. for c,

$$\mathrm{i}\,\dot{c}^{\alpha} = T^{\alpha} c^{\alpha} + V^{\alpha C}_e c^C, \qquad (\alpha = L, R), \quad (4)$$

$$\mathrm{i}\,\dot{c}^{C} = T^{C} c^C + V^{CL}_e c^L + V^{CR}_e c^R + [c^C, H_{epi}]. \quad (5)$$

We set $\hbar = 1$, $e = 1$ throughout the formulae. The lead operators can be solved formally,

$$c^{\alpha}(t) = \mathrm{i} g^r_{\alpha}(t, t_1) c^{\alpha}(t_1) + \int_{t_1}^{t} g^r_{\alpha}(t, t') V^{\alpha C}_e c^C(t')\, \mathrm{d}t', \quad (6)$$

where $g^r_{\alpha}(t, t') = -\mathrm{i}\theta(t - t')\langle [c^{\alpha}(t), c^{\dagger\alpha}(t')]_+ \rangle$ is the electron retarded Green's function for the lead α. It satisfies

$$\mathrm{i}\frac{\partial}{\partial t'} g^r_{\alpha}(t, t') + g^r_{\alpha}(t, t') T^{\alpha} = -I\delta(t - t'), \quad (7)$$

with the boundary condition $g^r_{\alpha}(t, t') = 0$ ($t < t'$). Using equation (6), the equation of motion of the central operator reads

$$\mathrm{i}\dot{c}^C = T^C c^C + \int_{t_1}^{t} \Sigma^r(t, t') c^C(t')\, \mathrm{d}t' + \xi + \sum_k M^k u_k c^C. \quad (8)$$

Similar equations can be derived for the phonon displacement operators [16],

$$\ddot{u}^C = -K^C u^C + F_n - \int_{t_1}^{t} \Pi^r(t, t') u^C(t')\, \mathrm{d}t' + \eta - c^{C\dagger} M c^C. \quad (9)$$

F_n is the force due to anharmonic effect. The last terms of equations (8) and (9) are due to EPI. We have only kept the first order term of the Taylor expansion, although inclusion of higher orders is straightforward. Equations (8) and (9) have the form of the generalized Langevin equation for the quantum Brownian motion [17].

Let us try to understand these two equations. The damping kernels $\Sigma^r = \Sigma^r_L + \Sigma^r_R$ and $\Pi^r = \Pi^r_L + \Pi^r_R$ are the electron and phonon retarded self-energies in the NEGF formalism. They are defined as, e.g. for electrons

$$\Sigma^r_{\alpha}(t, t') = V^{C\alpha}_e g^r_{\alpha}(t, t') V^{\alpha C}_e, \qquad (\alpha = L, R). \quad (10)$$

In the wide-band limit, the coupling with the leads does not depend on the energy. The damping kernel approaches the memoryless δ-function in the time domain. $\xi = \xi_L(t) + \xi_R(t)$ and $\eta = \eta_L(t) + \eta_R(t)$ are electron and phonon random noises due to the leads ($\alpha = L, R$)

$$\xi_{\alpha}(t) = \mathrm{i} V^{C\alpha}_e g^r_{\alpha}(t, t_1) c^{\alpha}(t_1), \quad (11)$$

and

$$\eta_{\alpha}(t) = V^{C\alpha}_{ph} \left[d^r_{\alpha}(t, t_1) \dot{u}^{\alpha}(t_1) - \dot{d}^r_{\alpha}(t, t_1) u^{\alpha}(t_1) \right]. \quad (12)$$

$d^r_{\alpha}(t, t_1) = -\mathrm{i}\theta(t - t_1)\langle [u^{\alpha}(t), u^{\alpha}(t_1)^T] \rangle$ is the lead retarded Green's function for phonons. In the leads the electron and phonon subsystems do not couple. They are both linear systems. In addition, the left and right leads do not interact directly. The statistical properties of the random noises are determined by the equilibrium ensembles at the remote pass, t_1. Working in the eigenmode representation, we can show that the expectation value of each noise term is zero. We can also obtain their correlation matrices, e.g. for electrons

$$\Xi^{\alpha}(t, t') = \langle \xi^{\dagger}_{\alpha}(t') \xi^T_{\alpha}(t) \rangle^T = -\mathrm{i}\Sigma^<_{\alpha}(t - t'). \quad (13)$$

As expected, it does not depend on the initial time t_1, and is time translationally invariant. It is convenient to work in the Fourier domain,

$$\tilde{\Xi}^{\alpha}[\omega] = \int_{-\infty}^{+\infty} \Xi^{\alpha}(t - t')\, \mathrm{e}^{\mathrm{i}\omega(t-t')}\, \mathrm{d}t = f^{\alpha}_e(\omega) \Gamma^{\alpha}_e[\omega]. \quad (14)$$

$f^{\alpha}_e(\omega)$ is the Fermi distribution function. $\Gamma^{\alpha}_e[\omega] = \mathrm{i}(\Sigma^r_{\alpha}[\omega] - \Sigma^a_{\alpha}[\omega])$ denotes the coupling with the leads. $\tilde{\Xi}^{\alpha}[\omega]$ is positive semi-definite, as required from a classical noise correlation. The phonon noise has a similar relation. A symmetric form is used here [16]

$$\tilde{F}^{\alpha}[\omega] = \tfrac{1}{2} \int_{-\infty}^{+\infty} \left(\langle \eta_{\alpha}(t) \eta^T_{\alpha}(t') \rangle + \langle \eta_{\alpha}(t') \eta^T_{\alpha}(t) \rangle^T \right) \mathrm{e}^{\mathrm{i}\omega(t-t')}\, \mathrm{d}t = \left(f^{\alpha}_{ph}(\omega) + \tfrac{1}{2} \right) \Gamma^{\alpha}_{ph}[\omega], \quad (15)$$

where $f^{\alpha}_{\rm ph}(\omega)$ is the Bose distribution for phonons, $\Gamma_{\rm ph}$ is similar to $\Gamma_{\rm e}$.

We notice that the noise equations (11) and (12) contain operators that satisfy anti-commutation or commutation relations. Electrons and phonons need different treatment. Equations (13) and (14) are only applicable to electrons. To study the hole transport, we need to use the correlation matrix $\langle \xi_\alpha(t)\xi^\dagger_\alpha(t')\rangle$. For phonons a symmetrization is needed to eliminate an imaginary part of the correlation. In both cases the relation between the damping and the noise term is a kind of manifestation of the quantum fluctuation-dissipation theorem.

The electrical and energy current can be obtained from different methods. We can use the current continuity condition. In the case of a discrete Hamiltonian, the electrical current from cell $j-1$ to cell j is, with only the lowest EPI term included,

$$I_j = -{\rm i}\Big(c^\dagger_j T_{j,j-1}c_{j-1} + \sum_k c^\dagger_j M^k_{j,j-1}c_{j-1}u_k - {\rm h.c.}\Big). \quad (16)$$

We can also get the current from each lead by studying the time derivative of the electron number

$$I_\alpha = -\frac{{\rm d}N_\alpha}{{\rm d}t} = -{\rm i}(c^{C\dagger}B_\alpha - {\rm h.c.}), \quad (17)$$

where $B_\alpha = V^{C\alpha}c^\alpha = \xi_\alpha + \int_{t_1}^t \Sigma^r_\alpha(t,t')c^C(t')\,{\rm d}t'$. In the same way, the electron energy current is

$$I^E_\alpha = -\frac{{\rm d}H_\alpha}{{\rm d}t} = -(B^\dagger \dot{c}^C + {\rm h.c.}). \quad (18)$$

So far the formal quantum Langevin equations are in terms of operators. To perform an MD simulation, we need to turn the operators into numbers. This is achieved by taking their quantum mechanical expectation values at the beginning of the dynamics. It is reasonable to assume that the central region and the two leads are decoupled at that time. The two baths assume canonical equilibrium distributions, and the central region is in an arbitrary state denoted by the density matrix ρ^C. The expectation value of any operator A^C is $\langle A^C\rangle = {\rm Tr}\{\rho^C A^C\}$. Taking the expectation value of these operators, generating the noise series using their correlations [16], the operator Langevin equations are turned into c-number equations. For products of operators, mean-field type approximation is used, e.g. $\langle cu\rangle \approx \langle c\rangle\langle u\rangle$. MD simulation can be done using these two equations. The final result is the ensemble average over the initial states. To evaluate the electrical current, the operators in equations (16)–(18) are replaced by the c-numbers obtained from MD simulation, and also $c^\dagger$ replaced by c^*, which is the complex conjugate of c. By doing this, we have taken the classical approximation to the operators.

One may cast doubt that this approximation may be too inaccurate to give reasonable results for the fermionic system for the electrical current. However, we can show rigorously that for the ballistic case the classical Langevin dynamics with the appropriate noises gives exactly the same result as that predicted by the NEGF method [14, 18, 19]. To do this, we define

$$-{\rm i}2\pi\delta(\omega-\omega')\mathcal{G}^<[\omega] \equiv \langle c^*[\omega']c^{\rm T}[\omega]\rangle^{\rm T}, \quad (19)$$

and

$${\rm i}2\pi\delta(\omega-\omega')\mathcal{G}^r[\omega]\Sigma^>_\alpha[\omega] \equiv \langle c[\omega]\xi^\dagger_\alpha[\omega']\rangle; \quad (20)$$

similarly for the phonon variables

$${\rm i}2\pi\delta(\omega-\omega')\mathcal{D}^<[\omega] \equiv \langle u^*[\omega']u^{\rm T}[\omega]\rangle^{\rm T}, \quad (21)$$

and

$${\rm i}2\pi\delta(\omega-\omega')\mathcal{D}^r[\omega]\Pi^>_\alpha[\omega] \equiv \langle u[\omega]\eta^\dagger_\alpha[\omega']\rangle. \quad (22)$$

We write equation (17) in the energy domain and substitute the equations (19) and (20) into it. After some rearrangement, we get exactly the Meir–Wingreen formula in the NEGF method. The only difference is that now the two Green's functions are defined as in equations (19) and (20). To further analyze the difference between the present method and the NEGF method, we write the Langevin equations in the frequency domain

$$c^C[\omega] = G^r_0[\omega]\left(\xi[\omega] + \int M^k u_k[\omega']c^C[\omega-\omega']\frac{{\rm d}\omega'}{2\pi}\right), \quad (23)$$

$$u^C[\omega] = D^r_0[\omega]\Bigg(-\eta[\omega] - F_n[\omega] + \int c^{C\dagger}[\omega]Mc^C[\omega-\omega']\frac{{\rm d}\omega'}{2\pi}\Bigg). \quad (24)$$

We also have

$$B_\alpha[\omega] = \xi_\alpha[\omega] + \Sigma^r_\alpha[\omega]c^C[\omega]. \quad (25)$$

In the ballistic case, we can see that $\mathcal{G}^<$ and $\mathcal{G}^r$ reduced to $G^<_0$ and G^r_0, which are the lesser and retarded Green's functions without EPI in the NEGF formula. The two methods are exactly the same. In the presence of EPI, equations (23) and (24) are coupled. Repeated iteration with respective to $c^C[\omega]$ and $u^C[\omega]$ gives an infinite series of terms. If we compare the lowest nonlinear terms in the quasi-classical approximation with that of the NEGF method, we find that the quasi-classical approximation only reproduces correctly part of the NEGF terms. That is out of the seven nonlinear self-energy graphs in the NEGF method, two of the graphs involving $G^>$ are replaced by $-\mathcal{G}^<$ in the quasi-classical approximation. This is because we do not have the (anti-)commutation relations for the Bose (Fermi) operators. These wrong terms are not important when the electron number per site in the center region is small or the EPI is not strong, which defines the application range of the quasi-classical approximation.

3. Numerical results and discussions

To illustrate the present approach, we take a simple one-dimensional (1D) atomic chain connected with two 1D leads and simulate the coupled equations (8) and (9) on a computer. Each atom has only one displacement degree of freedom and one spinless electron state. We take the two leads to be the same with spring constant $k_{\rm l}$, hopping matrix element $-h_{\rm l}$, and electron on-site energy $\varepsilon_{\rm l}$. $k_{\rm c}$, $-h_{\rm c}$, and $\varepsilon_{\rm c}$ denote those of the central part. Their couplings are $-v_{\rm e}$ and $-v_{\rm ph}$ for electrons

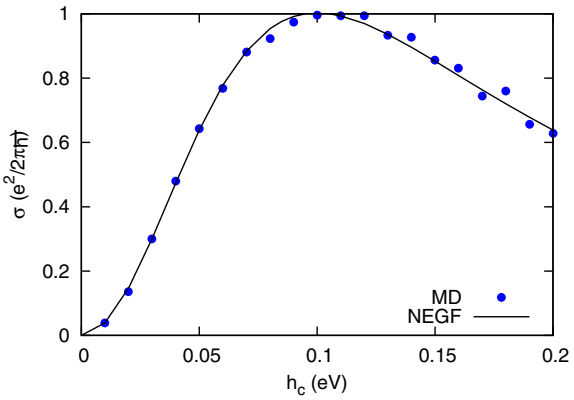

Figure 1. Ballistic electron quantum conductance as a function of the hopping matrix element between the two atoms h_c at 1 K. Other parameters are $\varepsilon_c = \varepsilon_l = 0$, $h_l = 0.1$ eV, $v_e = 0.1$ eV. The line is from NEGF and the dots are MD.

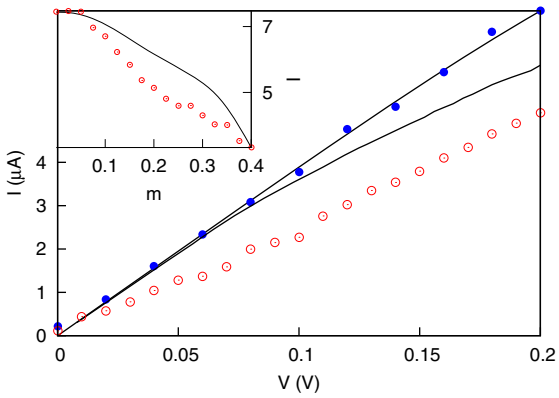

Figure 2. Current–voltage characteristics of the two-atom chain at 1 K with the following parameters: $h_l = 1.0$, $h_c = 0.1$ eV, $v_e = 0.32$ eV, $\varepsilon_c = \varepsilon_l = 0$, $k_l = k_c = 0.5$ eV/(amu Å^2), $v_{ph} = 0.1$ eV/(amu Å^2), and $m = 0.2$ eV/(amu$^{\frac{1}{2}}$ Å). A small on-site spring constant $k_0 = 0.2k_c$ is applied for the whole structure. MD results are shown as points and NEGF as lines. The filled dots and the straight line are the ballistic results. The lower line and the unfilled dots are results with EPI. The inset shows the electrical current as a function of EPI strength m at $V = 0.2$ V.

and phonons. Some of the matrices, e.g. T^C and V_e^{LC}, are given by

$$T^C = \begin{pmatrix} \varepsilon_c & -h_c & 0 & \cdots \\ -h_c & \varepsilon_c & -h_c & \cdots \\ 0 & -h_c & \varepsilon_c & -h_c \\ \cdots & 0 & -h_c & \varepsilon_c \end{pmatrix}, \tag{26}$$

$$V_e^{LC} = \begin{pmatrix} 0 & \cdots & & \\ 0 & 0 & \cdots & \\ -v_e & 0 & 0 & \cdots \end{pmatrix}. \tag{27}$$

The lead Green's functions have analytical solutions [11]. The anharmonic force F_n is turned off in order to perform a comparison with the NEGF method. The voltage is applied by shifting the chemical potentials of the two leads. A tight-binding Su–Schrieffer–Heeger type EPI term [20]

$$H_{epi} = m \sum_{i=1}^{L-1} \left(c_i^\dagger c_{i+1} + c_{i+1}^\dagger c_i\right)(u_{i+1} - u_i) \tag{28}$$

is used in the simulation. The Langevin equations, with all the operators replaced by their expectation values, are numerically solved using a fourth order Runge–Kutta method. A time-step of $\Delta t = 5 \times 10^{-17}$ s and 10^6 MD steps are used for each data point. As for the NEGF results, the Meir–Wingreen expression for electrical current [19], $I_\alpha = \frac{e}{2\pi} \int \mathrm{Tr}\{G^> \Sigma_\alpha^< - G^< \Sigma_\alpha^>\} \mathrm{d}\omega$, is used. The greater (lesser) self-energy $\Sigma_\alpha^>[\omega]$ ($\Sigma_\alpha^<[\omega]$) is due to the lead α. $G^>[\omega]$ ($G^<[\omega]$) is the greater (lesser) Green's function of the central region. A finite difference is used to calculate the quantum conductance from the electrical current.

We first demonstrate that the MD and the NEGF method give the same results in the ballistic case. Figure 1 shows the ballistic electron conductance of a two-atom chain as a function of the hopping matrix element between them h_c. When $h_c = 0.1$ eV, the conductance reaches a maximum value corresponding to one quantum unit ($e^2/2\pi\hbar$). The MD and the NEGF method give exactly the same results within the statistical errors of the MD simulation. This can also be seen from the ballistic I–V curve in figure 2 (the upper curve in the main panel).

Now we turn on the EPI. The main panel of figure 2 shows the I–V characteristics of the two-atom junction. The lower and upper curves are with and without EPI, respectively. In the presence of EPI, both methods give approximate results. The NEGF results are based on the SCBA, where only the non-crossed Feynman diagrams are included in the self-energies [11]. The MD method is non-perturbative and includes both crossed and non-crossed diagrams, but only part of these diagrams is treated correctly. As a result, the electrical current from MD is lower than that from the NEGF method. This can also be seen from the inset of figure 2 where we change the electron–phonon interaction strength at an applied bias of 0.2 V.

A detailed analysis of the high order terms in the quasi-classical approximation shows that its accuracy depends much on the electron average occupation number in the center region. When the electron number in small, the diagrams that the quasi-classical approximation treats incorrectly are not important. In this regime, the MD method should be accurate quantitative. Out of this regime, it can only give qualitative results. This analysis is confirmed in figure 3, where we show the electrical current and average electron number per atom as a function of the electron on-site energy in the center region. The electron number from the two methods shows slight discrepancy only when the on-site energy is very low. The MD electrical current agrees with the NEGF method only when the electron number is below 0.3.

The MD approach has its advantage: it can handle much larger systems than the NEGF method. This is easy to understand. Given the total degrees of freedom N, we only need to solve a set of $2N$ coupled equations in the MD method, while in the NEGF method matrix multiplication and inverse need much longer computer time (of order N^3). In figure 4, we show the length dependence of the electron conductance. Study of this effect using the NEGF method is formidable.

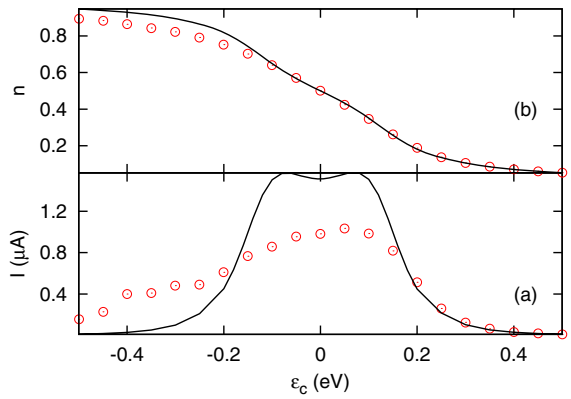

Figure 3. The electrical current I (a) and the average electron number per site n (b) at $V = 0.04$ V as a function of electron on-site energy ε_c in the center. The electron–phonon interaction $m = 0.2$ eV/(amu$^{\frac{1}{2}}$ Å). All other parameters are the same as in figure 2.

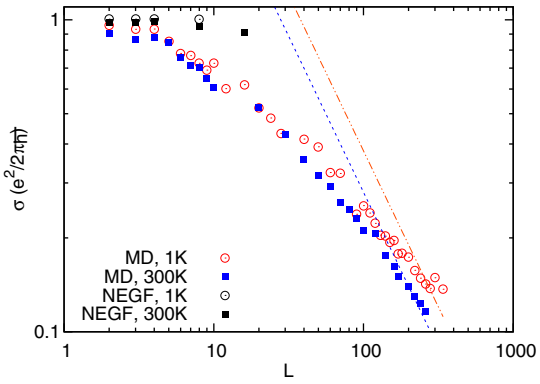

Figure 4. Log scale plot of the electron conductance as a function of chain length for $m = 0.05$ eV/(amu$^{\frac{1}{2}}$ Å), $h_l = h_c = v_e = 0.1$ eV, and $\varepsilon_c = \varepsilon_l = 0$. Phonon parameters are the same as in figure 2.

Besides the long computer time needed, convergence is also hard to achieve for long chains. From the log scale plot, we find a length independent conductance for short chains and close to inverse linear $(1/L)$ dependence for long chains. This corresponds to a ballistic to diffusive transition of the electronic transport. This transition takes place earlier at 300 K due to more available phonons for scattering. Previous study of this transition relied on a phenomenological method [21]. Thus a first-principle method that is able to cover both regions is highly desirable. The MD method proposed here could be one candidate.

The NEGF results should be valid at small values of EPI. But at intermediate interaction range, no good approximation exists. From this point of view, the MD method proposed here provides an alternative non-perturbative way to study the coupled electron–phonon dynamics in the intermediate EPI regime, although it is quantitatively accurate only when the electron occupation number is small. The MD method does not depend on the forms of the EPI Hamiltonian and the phonon anharmonic potential, though not exploited here. More importantly, it can handle much larger systems than the NEGF method. Further improvement of the results may be obtained by including higher order quantum corrections [9, 22].

4. Conclusions

In summary, we have proposed an MD method to study the coupled electron and phonon transport in open nonequilibrium molecular structures. It is based on the generalized quantum Langevin equations. The effects of the leads are reflected in the Langevin equations as noises and damping terms, which satisfy the quantum fluctuation-dissipation theorem. Quantum effects of the leads are taken into account properly at least for the electrical or energy current calculation. The method gives exact results for both electrons and phonons in the ballistic transport regime. When there is EPI, it is a quasi-classical approximation. The approximation is valid when the electron occupation number in the center region is small. The method shows its advantages in treating large systems, where a fully quantum mechanical study is formidable. We illustrate this by studying the ballistic to diffusive transition of the electrical conductance in 1D chains. Although only examples of electrical currents are presented here, it has other applications. For example, we can also study thermoelectric transport in molecular structures.

Acknowledgments

The authors thank Professor Per Hedegård, Professor Mads Brandbyge, Jian Wang, Lifa Zhang, and Yong Xu for discussions. This work was supported in part by a Faculty Research Grant (R-144-000-173-101/112) of the National University of Singapore.

References

[1] Galperin M, Ratner M A and Nitzan A 2007 *J. Phys.: Condens. Matter* **19** 103201
[2] Agraït N, Yeyati A L and van Ruitenbeek J M 2003 *Phys. Rep.* **377** 81
[3] Mitra A, Aleiner I and Millis A J 2004 *Phys. Rev.* B **69** 245302
[4] Frederiksen T, Brandbyge M, Lorente N and Jauho A-P 2004 *Phys. Rev. Lett.* **93** 256601
[5] Mahan G D 2000 *Many-Particle Physics* 3rd edn (Dordrecht: Kluwer, Academic/Plenum)
[6] Alexandrov A S and Bratkovsky A M 2007 *J. Phys.: Condens. Matter* **19** 255203
[7] Ness H and Fisher A J 1999 *Phys. Rev. Lett.* **83** 452
[8] Verdozzi C, Stefanucci G and Almbladh C O 2006 *Phys. Rev. Lett.* **97** 046603
[9] Horsfield A P, Bowler D R, Fisher A J, Todorov T N and Sánchez C G 2005 *J. Phys.: Condens. Matter* **17** 4793
[10] Galperin M, Nitzan A and Ratner M A 2007 *Phys. Rev.* B **75** 155312
[11] Lü J T and Wang J-S 2007 *Phys. Rev.* B **76** 165418
[12] Ford G W, Kac M and Mazur P 1965 *J. Math. Phys.* **6** 504
[13] Segal D, Nitzan A and Hänggi P 2003 *J. Chem. Phys.* **119** 6840
[14] Dhar A and Shastry B S 2003 *Phys. Rev.* B **67** 195405
[15] Schmid A 1982 *J. Low Temp. Phys.* **49** 609
[16] Wang J-S 2007 *Phys. Rev. Lett.* **99** 160601
[17] Hänggi P and Ingold G-L 2005 *Chaos* **15** 026105
[18] Caroli C, Combescot R, Nozieres P and Saint-James D 1971 *J. Phys. C: Solid State Phys.* **4** 916

[19] Jauho A.-P, Wingreen N S and Meir Y 1994 *Phys. Rev.* B **50** 5528
[20] Su W P, Schrieffer J R and Heeger A J 1979 *Phys. Rev. Lett.* **42** 1698
[21] Datta S 1997 *Electronic Transport in Mesoscopic Systems* (Cambridge: Cambridge University Press)
[22] Prezhdo O V and Pereverzev Y V 2000 *J. Chem. Phys.* **113** 6557